0013-7227/07/$15.00/0
Printed in U.S.A.

Endocrinology 148(9):4217–4225

doi: 10.1210/en.2007-0017

Regulation of Central Melanocortin Signaling by Interleukin-1β

Jarrad M. Scarlett, Erin E. Jobst,* Pablo J. Enriori,* Darren D. Bowe,* Ayesha K. Batra, Wilmon F. Grant, Michael A. Cowley, and Daniel L. Marks

Center for the Study of Weight Regulation and Associated Disorders (J.M.S., D.D.B., A.K.B., W.F.G., D.L.M.) and Department of Pediatrics (D.L.M.), Child Development and Rehabilitation Center, Oregon Health and Science University, Portland, Oregon 97239; Division of Neuroscience (E.E.J., P.J.E., M.A.C.), Oregon National Primate Research Center, Oregon Health and Science University, Beaverton, Oregon 97006; and School of Physical Therapy (E.E.J.), Pacific University, Hillsboro, Oregon 97123

Anorexia and involuntary weight loss are common and debilitating complications of a number of chronic diseases and inflammatory states. Proinflammatory cytokines, including IL-1β, are hypothesized to mediate these responses through direct actions on the central nervous system. However, the neural circuits through which proinflammatory cytokines regulate food intake and energy balance remain to be characterized. Here we report that IL-1β activates the central melanocortin system, a key neuronal circuit in the regulation of energy homeostasis. Proopiomelanocortin (POMC) neurons in the arcuate nucleus of the hypothalamus (ARC) were found to express the type I IL-1 receptor. Intracerebroventricular injection of IL-1β induced the expression of Fos protein in ARC POMC neurons but not in POMC neurons in the commissural nucleus of the tractus solitarius. We further show that IL-1β increases the frequency of action potentials of ARC POMC neurons and stimulates the release of α-MSH from hypothalamic explants in a dose-dependent fashion. Collectively, our data support a model in which IL-1β increases central melanocortin signaling by activating a subpopulation of hypothalamic POMC neurons and stimulating their release of α-MSH. (*Endocrinology* 148: 4217–4225, 2007)

ACTIVATION OF THE host immune system in response to tissue injury or infection triggers the release of proinflammatory cytokines that mediate a number of metabolic and behavioral responses including anorexia, pyrexia, and malaise (1, 2). This illness behavior is hypothesized to be elicited by cytokines exerting their actions on the central nervous system) (3, 4). Acutely, these responses represent an adaptive response that promotes survival of the host (5) but may become harmful if sustained. For example, short-term anorexia appears to promote survival because increased mortality occurs with forced feeding of animals suffering from illness (6). In contrast, prolonged anorexia, as occurs in animals with cachexia or disease-associated wasting, promotes increased morbidity and mortality (7). However, the means by which cytokines alter energy regulation and the relationship of cytokine signaling to neural systems previously shown to be involved in the regulation of energy homeostasis remains largely unknown.

The central melanocortin system plays a critical role in the regulation of food intake and energy homeostasis. This occurs principally via the action of melanocortin peptides derived from proopiomelanocortin (POMC) with a family of five G protein-coupled melanocortin receptors (MC1R–MC5R), and the endogenous melanocortin receptor antagonist agouti-related protein (AgRP) (8). In the mammalian brain, the central melanocortin system is comprised of adjacent populations of POMC- and AgRP/neuropeptide Y (NPY)-coexpressing neurons in the arcuate nucleus of the hypothalamus (ARC) and a caudal brainstem population of POMC neurons in the commissural nucleus of the tractus solitarius (NTS) (9, 10). Two melanocortin receptor subtypes, the melanocortin-3 receptor (MC3R) and MC4R, are expressed in the brain and are thought to be the primary mediators of the behavioral and metabolic effects of melanocortin peptides (8, 11). The ability of POMC and AgRP/NPY neurons to recognize and respond to a number of circulating signals of energy balance including leptin, insulin, and ghrelin strongly supports this system having a critical role in the regulation of energy homeostasis (12–14). Leptin, a 16-kDa protein resembling the structure of 4-α-helical bundle cytokines (15), acts through leptin receptors present on ARC POMC and AgRP/NPY neurons (16, 17) to suppress food intake and increase energy expenditure by increasing the release of α-MSH from POMC neurons and decreasing the release of NPY and AgRP (12). The responsiveness of the central melanocortin system to leptin raises the possibility that it may play a role in mediating the anorexic effects of additional cytokines.

The proinflammatory cytokine IL-1β is secreted by activated immune cells and plays a critical role in mediating the inflammatory response of the host against infection and tissue injury (18–20). Administration of IL-1β, peripherally or centrally, induces anorexia, fever, and activation of the hy-

First Published Online May 24, 2007

* E.E.J., P.J.E., and D.D.B. contributed equally to this work.

Abbreviations: aCSF, Artificial cerebrospinal fluid; AgRP, agouti-related protein; ARC, arcuate nucleus of the hypothalamus; EGFP, enhanced green fluorescent protein; icv, intracerebroventricular; IL-1R, IL-1 receptor; MC3R, melanocortin-3 receptor; NPY, neuropeptide Y; NTS, nucleus of the tractus solitarius; POMC, proopiomelanocortin.

***Endocrinology* is published monthly by The Endocrine Society (http://www.endo-society.org), the foremost professional society serving the endocrine community.**

pothalamo-pituitary-adrenal axis (19–21). Intracerebroventricular (icv) administration of the IL-1 receptor antagonist attenuates the anorexic effects of peripheral IL-1β and lipopolysaccharide administration (22). The effects of IL-1β in the brain are mediated by the type I IL-1 receptor (IL-1R) (23). Low to moderate levels of IL-1R mRNA are expressed by neurons in regions of the brain associated with energy homeostasis, including the ARC and brainstem (24). In previous work, IL-1β given iv to rats was shown to induce Fos protein in POMC mRNA-expressing neurons in the ARC, suggesting that the central melanocortin system may be a target for IL-1β signaling and have a role in mediating the behavioral effects of IL-1β (3). This hypothesis is strengthened by the observation that the anorexic effects of IL-1β can be blocked by central administration of a nonspecific melanocortin receptor antagonist (25).

In the present study, we report that IL-1β activates a subpopulation of POMC neurons in the ARC, but not in the NTS, and stimulates the release of α-MSH from hypothalamic explants in a dose-dependent manner. Our data also show that POMC neurons in the ARC express IL-1R mRNA. Collectively, our data support a model in which IL-1β increases central melanocortin signaling by activating a subpopulation of hypothalamic POMC neurons and stimulating them to release α-MSH.

Materials and Methods

Animals and surgical procedures

Male Sprague Dawley rats (300–350 g; Charles River Laboratories, Wilmington, MA), wild-type C57BL/6J mice (4–5 wk of age; Jackson Laboratory, Bar Harbor, ME), and transgenic C57BL/6J POMC-enhanced green fluorescent protein (EGFP) mice [6–8 wk of age; genotyping and breeding of mice were as described previously (26)] were maintained on a normal 12-h light, 12-h dark cycle with *ad libitum* access to food (Purina rodent diet 5001; Purina Mills, St. Louis, MO) and water. Experiments were conducted in accordance with the National Institutes of Health Guide for the Care and Use of Laboratory Animals and approved by the Animal Care and Use Committees of Oregon Health and Science University and the Oregon National Primate Research Center.

The icv cannulation and injections

Male POMC-EGFP mice were anesthetized with a ketamine cocktail and placed in a stereotaxic apparatus (Cartesian Instruments, Sandy, OR). A sterile guide cannula with obdurator stylet was stereotaxically implanted into the lateral ventricle (1.0 mm posterior to bregma, 0.5 mm lateral to midline, and 2.3 mm below the surface of the skull). The cannula was then fixed in place with dental cement. The animals were individually housed after surgery for a minimum of 1 wk and were handled and administered 1 μl icv injections of commercial artificial cerebrospinal fluid (aCSF) (Harvard Apparatus, Holliston, MA) daily. On the day of the experiment, mice were treated at 0900 h with 40 mg/kg ip ketorolac (K1136; Sigma-Aldrich, St. Louis, MO) dissolved in sterile saline or sterile saline. At 1000 h, mice received icv injections of 10 or 100 ng murine IL-1β (R&D Systems, Inc., Minneapolis, MN) dissolved in aCSF or aCSF alone. Ninety minutes after treatment, mice were deeply anesthetized and perfused transcardially with 0.9% saline followed by ice-cold 4% paraformaldehyde in 0.01 M PBS. Brains were postfixed for 2 h in fixative and then stored overnight in 20% sucrose in PBS as a cryoprotectant before being frozen at −80 C until use. The positions of the cannulas were verified at the end of the experiment by histological analysis.

Implantation of osmotic minipumps

ALZET micro-osmotic pumps (model 1007D; DURECT Corp., Cupertino, CA) were filled with ketorolac (K1136; Sigma-Aldrich) dissolved in sterile saline (n = 12) or sterile saline (n = 18). Ketorolac-filled pumps were calibrated to deliver a constant infusion of 1.0 mg/kg every 6 h. Male C57BL/6J mice were anesthetized with a ketamine cocktail, and the pumps were implanted sc on the dorsal surface of each mouse. Mice were allowed 2 d of recovery before use in hypothalamic peptide secretion studies.

Immunohistochemistry for c-Fos and EGFP

Dual-immunofluorescence histochemistry was performed as previously described (27). Briefly, free-floating sections were cut at 30 μm from perfused brains using a sliding microtome. Three sets of sections were generated from the hypothalamus and hindbrain of each brain. Hypothalamic sections were collected from the diagonal band of Broca (bregma 1.0 mm) caudally through the mammillary bodies (bregma −3.00 mm). Hindbrain sections were collected from the facial nucleus (bregma −5.75 mm) caudally through the spinal cord (28). The sections were incubated for 1 h at room temperature in blocking reagent (5% normal donkey serum in 0.01 M PBS and 0.3% Triton X-100). After the initial blocking step, the sections were incubated in rabbit anti-c-Fos antibody (PC38; EMD Biosciences, Inc., San Diego, CA) diluted 1:75,000 in blocking reagent for 48 h at 4 C, followed by incubation in 1:500 donkey antirabbit Alexa 594 (Molecular Probes, Inc., Eugene, OR) for 1 h at room temperature. Hindbrain sections were then incubated in rabbit anti-GFP antibody directly conjugated to Alexa 488 (Molecular Probes) diluted 1:4000 in blocking reagent for 1 h at room temperature. Hypothalamic sections did not require this step. Between each stage, the sections were washed thoroughly with 0.01 M PBS. Incubating the sections in the absence of primary antisera was used to ensure specificity of the secondary antibodies. Sections were mounted onto gelatin-coated slides, coverslipped using Vectashield mounting media (Vector Laboratories, Burlingame, CA), and viewed under a fluorescence microscope (Leica 4000 DM; Leica Microsystems, Bannockburn, IL).

Cell counting

The number of c-Fos-immunoreactive cells and double-labeled cells was counted by eye in sections representing the ARC and the NTS by investigators blinded to the treatments. Results are expressed as the number of cells per section as well as the percentage double-labeled. Each set of ARC sections contained seven to nine sections expressing immunopositive cells, and each set of caudal brainstem sections contained five to seven caudal brainstem sections expressing immunopositive cells. A cell was determined to be single-labeled when visible only under the fluorescence filter corresponding to the emission wavelength of the primary/secondary antibody complex used (*e.g.* 594 nm and not 488 nm for c-Fos). Cells were examined at multiple focal planes within the section and at multiple magnifications to ensure that the cell was indeed representative of a single-labeled cell. When the cell was visible at both 594- and 488-nm filters, it was deemed to be double-labeled. Double-labeled cells were examined at multiple focal planes within the section and at multiple magnifications to ensure that the cell was indeed representative of a single cell labeled with both antibody complexes and not two single-labeled cells in close proximity within different levels of the optical section. The cells were also examined under a third wavelength (350 nm) not corresponding to the emission wavelength of either of the secondary antibodies to ensure that the immunoreactivity was specific.

Electrophysiology

Standard electrophysiological techniques were used, as previously described (26). Briefly, 8-wk-old male POMC-EGFP mice were anesthetized with isoflurane and killed quickly by decapitation. Coronal hypothalamic slices containing the ARC were cut at 185 μm with a vibrating slicer (Leica VT1000S) under ice-cold aCSF solution of the following composition (in mM): 126 NaCl, 2.5 KCl, 1.2 $MgCl_2/6H_2O$, 2.4 $CaCl_2/2H_2O$, 1.2 NaH_2PO_4/H_2O, 21.4 $NaHCO_3$, and 11.1 glucose (saturated with 95% O_2/5% CO_2). Slices were stored for at least 1 h in a holding chamber with aCSF at room temperature and continuously bubbled with 95% O_2/5% CO_2. Individual slices were submerged in a recording chamber and superfused continuously with carbogenated aCSF at 35 C (3–5 ml/min). All recordings were made from ARC POMC

neurons, identified by bright green fluorescence (26). Electrode resistances were 2–4 MΩ when filled with an intracellular solution of the following composition (in mM): 128 K-gluconate, 10 HEPES, 1 EGTA, 10 KCl, 1 $MgCl_2$, 0.3 $CaCl_2$, 5 (Mg)ATP, 0.3 (Na)GTP. Current-clamp recordings were performed in whole-cell configuration with an Axopatch 200B amplifier (Axon Instruments, Foster City, CA). Data were filtered at 2 kHz and then sampled at 50–100 kHz by pClamp 8.2 software (Axon Instruments). Data were stored on a hard disk for analysis using Mini Analysis (Synaptosoft, Inc., Decatur, GA). Only neurons with stable holding currents not exceeding 100 pA for the 10-min baseline were studied. Approximately 10 min of baseline data were recorded for each arcuate neuron before drug application. Murine IL-1β (R&D Systems) was applied at specified concentrations to the superfusion medium by gravity perfusion for approximately 3 min, and data were recorded for approximately 15 min after drug was discontinued. All data are presented as mean ± SEM. Differences in drug effects were tested by either a one-sample Student's *t* test with a hypothetical mean of 0 mV (membrane potential) or with Student's *t* test (firing rate). For drug-induced changes in firing rate, changes are normalized to the 5-min period immediately before drug application. Only cells with a minimum average of five action potentials per 20-sec bin during baseline were included in the analysis to avoid the potential of overestimating changes in firing rate with extremely low-firing cells.

Hypothalamic peptide secretion

Male C57BL/6J mice (n = 30) were anesthetized with isoflurane and killed quickly by decapitation. The brain was removed (with care taken to ensure that there was no contamination of the hypothalamic portion with residual pituitary), and a 2-mm slice was prepared using a vibrating microtome (Leica VS 1000) to include the paraventricular and arcuate nuclei. Individual hypothalami received a 1-h equilibration period with aCSF [126 mM NaCl, 0.09 mM Na_2HPO, 6 mM KCl, 4 mM $CaCl_2$, 0.09 mM $MgSO_4$, 20 mM $NaHCO_3$, 8 mM glucose, 0.18 mg/ml ascorbic acid, and 0.6 trypsin inhibitory unit (TIU) aprotinin/ml] at 37 C. Hypothalami were then incubated for 45 min at 37 C in 700 μl aCSF (basal period) before being challenged with a single concentration of murine IL-1β (R&D Systems) (0.0001–1.0 nM) in 700 μl aCSF for 45 min at 37 C. Tissue viability was verified by a 45-min exposure to 700 μl aCSF containing 56 mM KCl. Treatments were performed in quadruplicate. At the end of each treatment period, supernatants were removed and frozen at −80 C until assayed by RIA. Hypothalamic explants that failed to show peptide release three times above that of basal in response to aCSF containing 56 mM KCl were excluded from data analysis.

Hypothalamic peptide secretion after ketorolac treatment

Male C57BL/6J mice that had been implanted with ketorolac-filled (n = 12) or saline-filled osmotic pumps (n = 18) were divided into five groups of six animals each. Mice from all groups were anesthetized with isoflurane and killed quickly by decapitation. Brains were removed and processed on a vibrating microtome as described above. Individual hypothalami received a 1-h equilibration period with aCSF at 37 C. A single group of hypothalami from mice that received saline pumps (n = 6) were incubated for 45 min at 37 C in 700 μl aCSF plus ketorolac (121 μM) (basal period) before being challenged with 0.1 nM murine IL-1β in 700 μl aCSF plus ketorolac (121 μM) for 45 min at 37 C. Hypothalami from the remaining four groups were incubated for 45 min at 37 C in 700 μl aCSF (basal period) before being challenged with either 0.05 nM (n = 6 for saline and ketorolac-treated mice) or 0.1 nM (n = 6 for saline and ketorolac-treated mice) murine IL-1β in 700 μl aCSF for 45 min at 37 C. Tissue viability was verified by a 45-min exposure to 700 μl aCSF containing 56 mM KCl. Treatments were performed in quadruplicate. At the end of each treatment period, supernatants were removed and frozen at −80 C until assayed by RIA. Hypothalamic explants that failed to show peptide release three times above that of basal in response to aCSF containing 56 mM KCl were excluded from data analysis.

α-MSH RIA

α-MSH immunoreactivity was measured with a rabbit anti-α-MSH specific for α-MSH (Phoenix Pharmaceuticals, Inc., Belmont, CA). The antibody cross-reacts fully with the mature α-MSH (*N*-acetylated α-MSH), and partially (46%) with desacetylated α-MSH, but not with NPY or AgRP. ^{125}I-labeled α-MSH was prepared by the iodogen method and purified by high-pressure liquid chromatography (University of Mississippi Peptide Radioiodination Service Center, University, MS). All samples were assayed in duplicate. The assay was performed in a total volume of 350 μl 0.06 M phosphate buffer (pH 7.3) containing 1% BSA. The sample was incubated for 3 d at 4 C before the separation of free and antibody-bound label by goat antirabbit IgG serum (Phoenix Pharmaceuticals). One hundred microliters of supernatant were assayed. The lowest detectable level that could be distinguished from the zero standard was 0.30 fmol/tube. The intraassay coefficient of variation was determined by replicate analysis (n = 10) of two samples at α-MSH concentrations of 2 and 10 fmol/tube, and the results were 7.8 and 7.5%, respectively. The interassay coefficients of variation were 10.7 and 12.1% for the range of values measured.

Double-label in situ hybridization histochemistry

Simultaneous visualization of POMC and IL-1R mRNA in the rat brain (n = 3) was performed as previously reported (29), with slight modifications. Coronal sections (20 μm) were cut on a cryostat and thaw-mounted onto Superfrost Plus slides (VWR Scientific, West Chester, PA). Hypothalamic sections were collected in a 1:6 series from the diagonal band of Broca (bregma 0.50 mm) caudally through the mammillary bodies (bregma −5.00 mm). Hindbrain sections were collected in a 1:6 series from the facial nucleus (bregma −10.00 mm) caudally through the spinal cord (30). Antisense ^{33}P-labeled rat IL-1R riboprobe (corresponding to bases 207–930 of rat IL-1R; GenBank accession no. M95578) (0.2 pmol/ml) and antisense digoxigenin-labeled rat POMC riboprobe (corresponding to bases 49–644 of rat POMC; GenBank accession no. AF510391) (concentration determined empirically) were denatured, dissolved in hybridization buffer along with tRNA (1.7 mg/ml), and applied to slides. Controls used to establish the specificity of the IL-1R riboprobe included slides incubated with an equivalent concentration of radiolabeled sense IL-1R riboprobe or radiolabeled antisense probe in the presence of excess (1000×) unlabeled antisense probe. Slides were covered with glass coverslips, placed in a humid chamber, and incubated overnight at 55 C. The following day, slides were treated with RNase A and washed under conditions of increasing stringency. The sections were incubated in blocking buffer and then in Tris buffer containing antidigoxigenin fragments conjugated to alkaline phosphatase (Roche Molecular Biochemicals, Indianapolis, IN), diluted 1:250, for 3 h at room temperature. POMC cells were visualized with Vector Red substrate (SK-5100; Vector Laboratories) according to the manufacturer's protocol. Slides were dipped in 100% ethanol, air dried, and then dipped in NTB-2 liquid emulsion (Eastman Kodak Co., Rochester, NY). Slides were developed 13 d later and coverslipped. Determination of cells expressing both IL-1R and POMC mRNA was performed using criteria previously described (29). Briefly, POMC-mRNA-containing cells were identified under fluorescent illumination, and custom-designed software was used to count the silver grains (corresponding to radiolabeled IL-1R mRNA) over each cell. Signal-to-background ratios for individual cells were calculated; an individual cell was considered to be double-labeled if it had a signal-to-background ratio of 2.5 or more. For each animal, the amount of double-labeling was calculated as a percentage of the total number of POMC-mRNA-expressing cells and then averaged across animals to produce mean ± SEM.

Statistical analysis

Data are expressed as mean ± SEM for each group. Statistical analysis was performed using SPSS (version 14.0) and Prism (version 3.03) software. All data were analyzed with a one-sample *t* test (electrophysiology data), an unpaired *t* test (immunohistochemistry data), one-way ANOVA followed by a *post hoc* analysis using a Bonferroni corrected *t* test (c-Fos with ketorolac data), or a two-way ANOVA followed by a one-way ANOVA with *post hoc* analysis using a Bonferroni multiple comparison test (secretion study with ketorolac). For all analyses, significance was assigned at the $P < 0.05$ level.

Results

IL-1β selectively activates c-Fos expression in ARC POMC-EGFP neurons

To test whether IL-1β activates ARC and NTS POMC-EGFP neurons, we examined the expression of c-Fos in POMC-EGFP neurons after icv injection of IL-1β. In agreement with the literature, icv administration of IL-1β (10 ng) induced c-Fos immunoreactivity in the ARC (aCSF, 21 ± 2 cells per section, n = 4; IL-1β, 79 ± 2 cells per section, n = 5; $P < 0.0001$) (Fig. 1, B, E, H, and J) and NTS (aCSF, 3 ± 1 cells per section, n = 4; IL-1β, 49 ± 5 cells per section, n = 4; $P < 0.0001$) (Fig. 2, B, E, and J). In the ARC, few POMC-EGFP neurons expressed c-Fos in aCSF-treated animals (7 ± 2% coexpression) (Fig. 1, C and K). IL-1β increased the c-Fos expression in ARC POMC-EGFP neurons by about 4-fold (31 ± 2% coexpression, $P < 0.0001$) (Fig. 1, F, I, and K). No additional increase in the number of POMC-EGFP neurons activated by IL-1β was observed when higher doses (100 ng) of IL-1β were administered (data not shown). In contrast to the arcuate POMC-EGFP neurons, NTS POMC-EGFP neurons were unresponsive to IL-1β. Expression of c-Fos by NTS POMC-EGFP neurons was very low in aCSF-treated animals (2 ± 0.5% coexpression) (Fig. 2, F and K) and remained low after IL-1β treatment (3 ± 0.5% coexpression, $P > 0.05$) (Fig. 2, F, I, and K).

Activation of ARC POMC-EGFP neurons by IL-1β is decreased by inhibition of cyclooxygenase activity

To determine whether the synthesis of prostaglandin intermediates is necessary for the activation of ARC POMC neurons by IL-1β, we examined the expression of c-Fos in ARC POMC-EGFP neurons from mice that had received an ip injection of ketorolac (40 mg/kg) or saline 1 h before receiving an icv injection of IL-1β (10 ng) or aCSF. The overall expression of c-Fos immunoreactivity in the ARC of mice that received IL-1β was significantly reduced in animals that had received ip ketorolac compared with animals that had received an ip injection of saline (saline, 45 ± 2 cells per section, n = 4; ketorolac, 25 ± 1 cells per section, n = 6; $P < 0.001$) but was still significantly increased compared with animals that had received ketorolac and an icv injection of aCSF (18 ± 1 cells per section, n = 4; $P < 0.01$) (Fig. 3A). As before, the expression of c-Fos in ARC POMC-EGFP neurons was increased by icv IL-1β in animals that had received ip saline injections (aCSF, 10 ± 1% coexpression, n = 4; IL-1β, 23 ± 1% coexpression, n = 4; $P < 0.001$) (Fig. 3B). Pretreatment with ketorolac reduced the expression of c-Fos in ARC POMC-EGFP neurons after IL-1β treatment (ketorolac, 16 ± 1% coexpression, n = 6; saline, 23 ± 1% coexpression, n = 4; $P < 0.01$) but failed to completely attenuate activation compared with animals that had received ip saline and icv aCSF ($P > 0.05$) (Fig. 3B).

IL-1β increases the firing rate of ARC POMC-EGFP neurons

Using EGFP-labeled cells in ARC slices from male POMC-EGFP mouse brains, we observed that bath-applied IL-1β (1 nM) depolarized 11 of 15 (73%) POMC-EGFP neurons tested (2.5 ± 0.9 mV; $P < 0.05$, one-sample Student's t test). In four of 15 (27%) POMC-EGFP neurons tested, IL-1β induced a small hyperpolarization (1.2 ± 0.1 mV; $P < 0.05$, one-sample Student's t test).

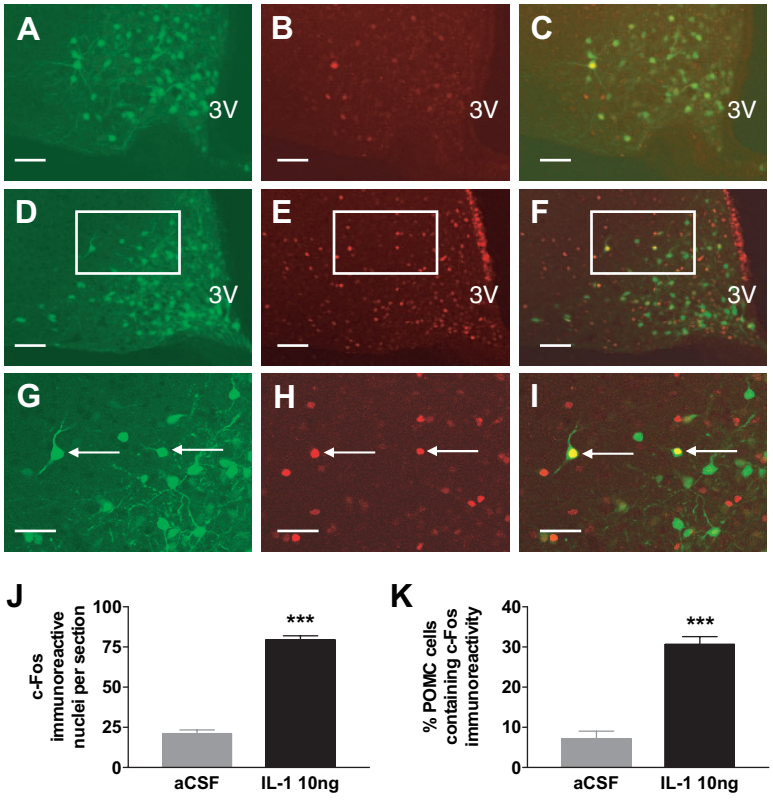

FIG. 1. IL-1β activates POMC-EGFP neurons in the hypothalamus. A, D, and G, Expression of EGFP in the hypothalamus of POMC-EGFP mice; B, expression of c-Fos (*red*) in aCSF-treated animals (icv, n = 4) is low; C, few POMC neurons express c-Fos after aCSF treatment. E and H, expression of c-Fos in IL-1β-treated animals (10 ng, icv, n = 5) is increased; F and I, IL-1β activates c-Fos in POMC neurons; G, H, and I, enlargement of D–F shown for clarity (*white boxes* denote regions of enlargement); J, IL-1β increases the expression of c-Fos in the ARC by about 3.5-fold (two-tailed Student's t test; ***, $P < 0.0001$ *vs.* aCSF); K, about 30% of POMC neurons are activated by icv IL-1β (10 ng, two-tailed Student's t test; ***, $P < 0.0001$ *vs.* aCSF). *Scale bars*, 65 μm (A–F) and 60 μm (G–I). 3V, Third ventricle.

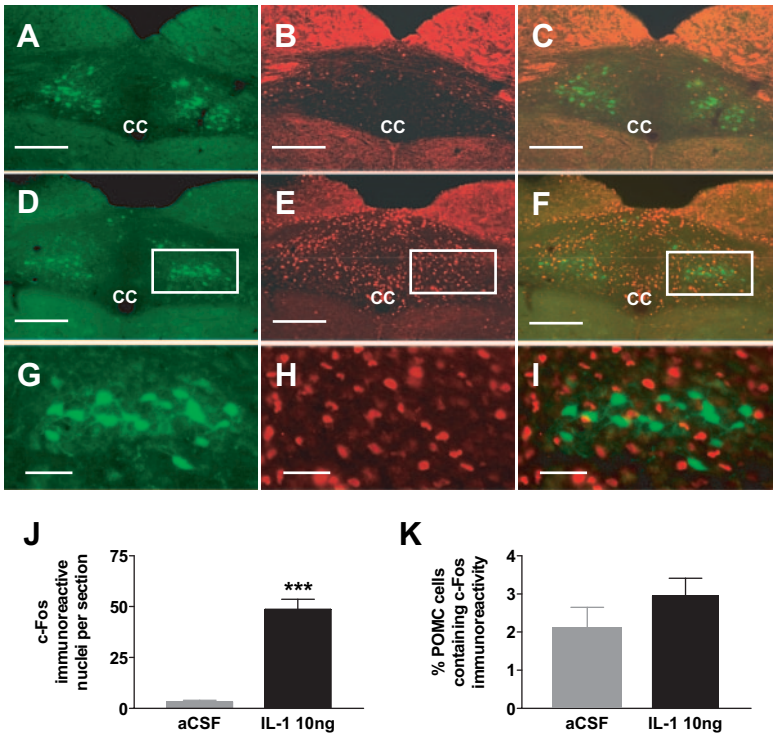

FIG. 2. IL-1β does not activate POMC-EGFP neurons in the NTS. A, D, and G, Expression of EGFP in the NTS of POMC-EGFP mice; B, expression of c-Fos (*red*) in aCSF-treated animals (icv, n = 4) is very low; F, few POMC neurons express c-Fos after aCSF treatment; E and H, expression of c-Fos in IL-1β-treated animals (10 ng, icv, n = 4) is increased; F and I, IL-1β does not activate c-Fos in POMC neurons; G–I, enlargements of D–F shown for clarity (*white boxes* denote regions of enlargement); J, IL-1β increases the expression of c-Fos in the NTS by about 16-fold (two-tailed Student's *t* test, ***, $P < 0.0001$ *vs.* aCSF); K, IL-1β does not increase the number POMC neurons activated in the NTS (two-tailed Student's *t* test, *P* value nonsignificant *vs.* aCSF). *Scale bars*, 100 μm (A–F) and 60 μm (G–I). CC, Central canal.

Of the spontaneously firing POMC-EGFP neurons (12 of 15 tested), IL-1β (1 nM) increased the firing frequency of 10 cells (83%) (Fig. 4A). To avoid overestimation of drug-induced increases in firing rate that occurs if extremely low-firing cells are assessed, two cells were excluded from analysis. IL-1β increased the firing rate 78.8 ± 12.1% from baseline to the 10-min washout period (n = 8; $P < 0.0001$) (Fig. 4B). During its peak effect during the first 250 sec after IL-1β addition to the bath (Fig. 4B), IL-1β increased POMC-EFGP neuronal activity by 87.4 ± 15.4% above baseline ($P < 0.0001$).

IL-1β stimulates the release of α-MSH from murine hypothalamic explants

To investigate the effect of IL-1β on α-MSH release *in vitro*, hypothalamic explants harvested from male C57BL/6 mice were incubated with IL-1β (0.01, 0.1, 1.0, 3.0, and 30.0 nM; n = 4 per IL-1β dose). These doses were chosen based on previous work estimating basal IL-1β concentration in the hypothalamus at 0.01–0.02 nM and increasing approximately 10-fold during pathological conditions (31). IL-1β significantly increased the release of α-MSH from hypothalamic

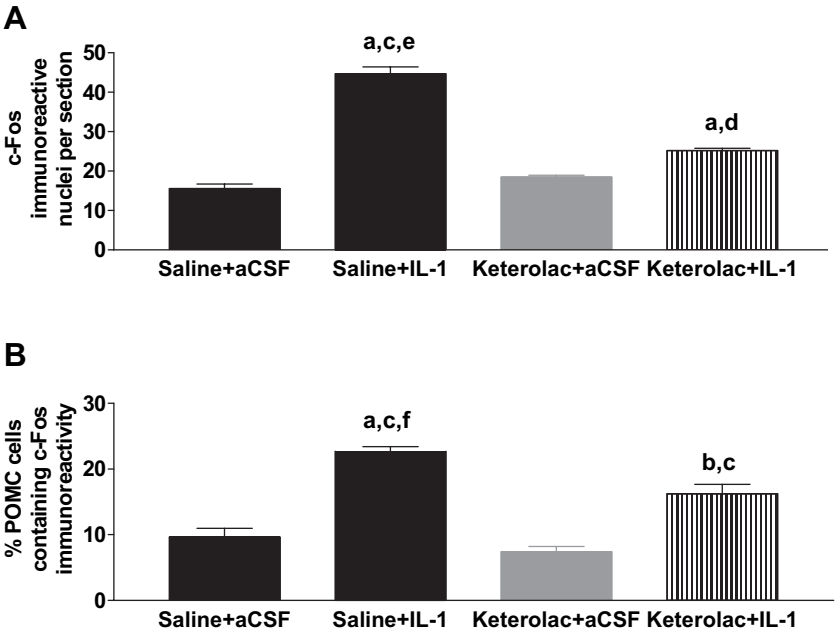

FIG. 3. Ketorolac reduces IL-1β activation of POMC-EGFP neurons in the hypothalamus. A, Expression of c-Fos in the ARC of POMC-EGFP mice receiving ip ketorolac (40 mg/kg) or saline followed by icv injection of IL-1β (10 ng) or aCSF 1 h later (saline + aCSF, n = 4; saline + IL-1β, n = 4; ketorlac + aCSF, n = 4; ketorolac + IL-1β, n = 6); B, reduced expression of c-Fos in ARC POMC-EGFP neurons in mice receiving ip ketorolac (40 mg/kg) or saline followed by icv injection of IL-1β (10 ng) or aCSF 1 h later (saline + aCSF, n = 4; saline + IL-1β, n = 4; ketorlac + aCSF, n = 4; ketorolac + IL-1β, n = 6). Data are expressed as mean ± SEM, and statistics were calculated by one-way ANOVA followed by a *post hoc* analysis using a Bonferroni corrected *t* test; a, $P < 0.001$ *vs.* saline + aCSF; b, $P < 0.01$ *vs.* saline + aCSF; c, $P < 0.001$ *vs.* ketorolac + aCSF; d, $P < 0.01$ *vs.* ketorolac + aCSF; e, $P < 0.001$ *vs.* ketorolac + IL-1; f, $P < 0.01$ *vs.* ketorolac + IL-1.

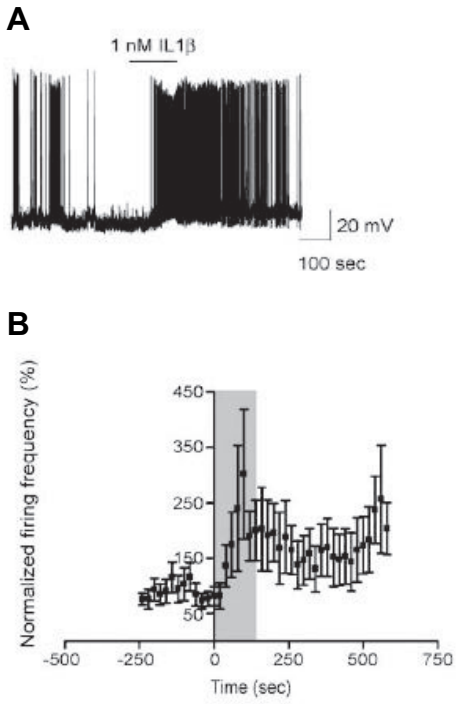

FIG. 4. IL-1β increases the firing rate of ARC POMC-EGFP neurons. A, Example of raw data (15-min trace) showing bath application of IL-1β (1 nM). IL-1β depolarized and increased spontaneous activity of a single ARC POMC-EGFP neuron. The mean of the membrane potential 5 min before IL-1β application was −54.5 mV; during application (2.32 min), it was −51.4 mV. The mean peak depolarization (from 1.5 min after start of drug application to 3.5 min into washout) was −45.6 mV. The mean firing frequency 5 min before IL-1β application was 0.52 Hz; during application, it was 1.86 Hz; and 5 min into washout period, it was 1.48 Hz. B, IL-1β (1 nM) increases the firing rate of ARC POMC-EGFP neurons (n = 8; $P < 0.0001$, baseline compared with washout). *Shaded region* corresponds to time of IL-1β addition to bath. *Error bars* represent SEM.

explants with a calculated EC_{50} of 5.9×10^{-11} M (Fig. 5). These results demonstrate that *in vivo* hypothalamic concentrations of IL-1β that are produced during pathological conditions are able to potently stimulate the *in vitro* release of α-MSH from hypothalamic explants.

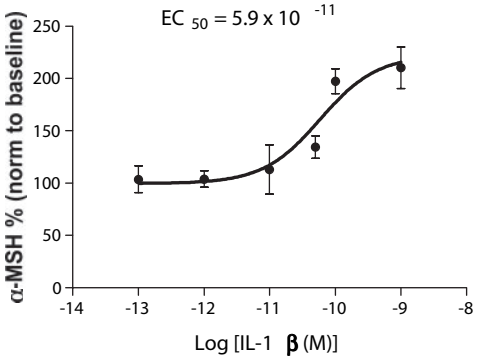

FIG. 5. IL-1β stimulates *in vitro* release of α-MSH from murine hypothalamic explants in dose-dependent manner with a calculated EC_{50} of 5.9×10^{-11} M. Values are means ± SEM (n = 4 for each dose).

Ketorolac treatment does not block IL-1β-stimulated release of α-MSH from murine hypothalamic explants

To determine whether inhibition of prostaglandin synthesis would reduce the IL-1β-stimulated release of α-MSH from hypothalamic explants, we repeated our explant studies using two doses of IL-1β (0.05 and 0.1 nM) in the presence of ketorolac. We observed that acutely blocking prostaglandin synthesis by incubating the explants in aCSF containing ketorolac (121 μM) did not alter either basal or IL-1β-stimulated α-MSH release ($P < 0.01$ *vs.* aCSF) (Fig. 6). To investigate the effects of chronic blockade of prostaglandin synthesis on IL-1β-stimulated α-MSH release, we implanted osmotic pumps containing either ketorolac or saline 2 d before the explant study. Both doses of IL-1β stimulated α-MSH release from hypothalamic explants from mice that had received saline-filled pumps, although only the higher dose of 0.1 nM reached significance ($P < 0.001$ *vs.* aCSF) (Fig. 6). Mice with ketorolac-filled pumps had reduced α-MSH release in response to both doses of IL-1β used compared with mice with saline pumps. However, this reduction did not achieve statistical significance for either dose of IL-1β ($P > 0.05$ *vs.* saline pump groups), and α-MSH release was still significantly increased in animals that had received ketorolac pumps at the high dose of IL-1β ($P < 0.05$ *vs.* aCSF) (Fig. 6). No significant interaction was found between method of infusion and dose of IL-1β by two-way ANOVA.

POMC mRNA coexpression with IL-1R mRNA in the hypothalamus

Hypothalamic sections from rat brains were processed for double-label *in situ* hybridization for POMC and IL-1R. The pattern of silver grain clusters representing cells in the ARC expressing IL-1R mRNA was similar to that previously reported with a radiolabeled probe (24) (Fig. 7A). Including excess unlabeled antisense probe with radiolabeled antisense probe abolished all specific signal, and no signal was seen

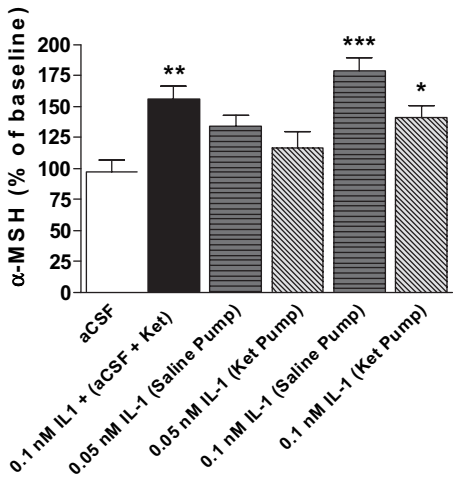

FIG. 6. Acute and chronic ketorolac treatment does not reverse IL-1β-stimulated *in vitro* release of α-MSH from murine hypothalamic explants. Data are expressed as mean ± SEM (n = 6 for each dose), and statistics were calculated by one-way ANOVA followed by a *post hoc* analysis using a Bonferroni multiple comparison test; *, $P < 0.05$ *vs.* aCSF; **, $P < 0.01$ *vs.* aCSF; ***, $P < 0.001$ *vs.* aCSF.

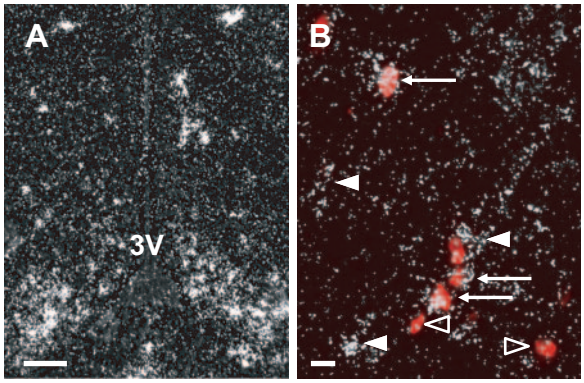

FIG. 7. Coexpression of POMC mRNA and IL-1R mRNA in the hypothalamus. A, Representative dark-field photomicrograph showing distribution of IL-1R mRNA (*white silver grain clusters*) in the ARC of wild-type rats; B, double-label *in situ* hybridization revealed clusters of silver grains representing IL-1R mRNA-expressing cells overlying ARC POMC mRNA-expressing neurons (*red precipitate*). *Arrows* point to POMC neurons that coexpress IL-1R mRNA. *Open arrowheads* represent POMC neurons that do not coexpress IL-1R mRNA. *Arrowheads* represent silver grain clusters not overlying POMC neurons. *Scale bars*, 300 μm (A) and 70 μm (B). 3V, Third ventricle.

with application of radiolabeled sense probes. A number of POMC mRNA-expressing neurons in the ARC, represented by cell bodies filled with fluorescent red precipitate, had overlying clusters of silver grains, signifying coexpression of IL-1R mRNA (Fig. 7B). Semiquantitative image analysis revealed that with a signal-to-background ratio of 2.5 set as the threshold for neurons to be considered double-labeled, 35 ± 7% of the digoxigenin-labeled POMC neurons coexpressed IL-1R mRNA. Technical limitations in obtaining consistent labeling of POMC neurons in the NTS using digoxigenin-labeled riboprobes prevented a thorough repetition of these studies in the NTS. However, in instances in which POMC neurons in the NTS were successfully labeled using digoxigenin-labeled riboprobes, no coexpression with IL-1R mRNA was observed (not shown).

Discussion

Both obesity and cachexia of chronic disease are known to be associated with increases in the circulating levels of proinflammatory cytokines (32, 33). Therefore, understanding how these cytokines interact with and regulate central feeding circuits is critical to our overall understanding of these disorders of energy balance. Data from a number of previous studies strongly suggested that the central melanocortin system might play a significant role in mediating the anorexic effects of IL-1β. Elevated cellular activity in ARC POMC neurons, as indicated by an increase in c-Fos expression, has been shown to occur in rats after IL-1β administration (3). Furthermore, the anorexic effects of IL-1β can be attenuated by central administration of either a mixed MC3R/MC4R antagonist (SHU9119) (25) or a MC4R-selective small-molecule antagonist (34). However, a comprehensive investigation of the sensitivity of the entire central melanocortin system to IL-1β and a characterization of the role of IL-1β in the biosynthesis and release of α-MSH from POMC neurons is lacking. In the present study, we report that ARC POMC neurons express IL-1R and that IL-1β selectively activates ARC POMC neurons. We further demonstrate that in acute hypothalamic slices, IL-1β depolarizes and increases the frequency of action potentials of ARC POMC neurons. In hypothalamic explants, IL-1β stimulates the release of α-MSH in a dose-dependent fashion. These findings suggest that IL-1β increases signaling at melanocortin receptors by targeting ARC POMC neurons and stimulating the release of α-MSH.

Our data suggest that ARC POMC neurons are distinct from NTS POMC neurons, in that arcuate POMC neurons are responsive to IL-1β as measured by the expression of c-Fos. One explanation for our inability to observe activation of NTS POMC neurons might be because of our central injections of IL-1β not stimulating vagal nerve afferents to the NTS. This possibility is reinforced by data that support a role for viscerosensory afferents of the vagus nerve mediating the responsiveness of NTS neurons to peripheral administration of compounds, including IL-1β (35). Indeed, cholecystokinin-sensitive vagal afferents have been shown to directly activate NTS POMC-EGFP neurons (36). However, neurons in the brains of vagotomized animals retain sensitivity to central injections of IL-1β (37), indicating that the absence of IL-1β-mediated vagal signaling is an unlikely explanation for our observed lack of POMC neuron activation in the NTS.

The expression of IL-1R mRNA by a subset of ARC POMC neurons indicates that these neurons may be direct targets for the actions of IL-1β. Our observation that some, but not all, ARC POMC neurons express IL-1R suggests that only a distinct subset of neurons participate in IL-1β-mediated signaling. This hypothesis is supported by our observation that only 31 ± 2% of POMC neurons express c-Fos in response to IL-1β. However, recordings from ARC POMC neurons also revealed that IL-1β induces a small hyperpolarization in 27% of POMC neurons tested. Although the physiological relevance of this hyperpolarization is unknown, it suggests that the population of POMC neurons that express c-Fos after IL-1β administration may represent only a fraction of the total ARC POMC population that participates in IL-1β-mediated signaling. In addition, the expression of IL-1R mRNA by ARC POMC neurons does not conclusively demonstrate that IL-1β acts directly upon ARC POMC neurons. Indirect mechanisms of IL-1β-mediated regulation of ARC POMC neuronal activity remain a strong possibility. We observed that ARC POMC neurons represented a minority population of cells that expressed IL-1R mRNA in the ARC. However, ARC POMC neurons not expressing IL-1R mRNA frequently had IL-1R mRNA-expressing cells of unknown phenotype directly adjacent to them. Data from previous studies suggest that many of the neural responses to IL-1β are mediated by the synthesis of endogenous prostaglandins. Blockade of prostaglandin synthesis with cyclooxygenase inhibitors or deletion of the *Ptges* gene that encodes for microsomal prostaglandin E synthase-1, the inducible terminal enzyme in the PGE2 synthesizing pathway, attenuates important components of the IL-1β-induced systemic response including hypothalamo-pituitary-adrenal activation (38) and anorexia (39). Indeed, IL-1β-mediated depolarization of magnocellular neurons in the paraventricular nucleus occurs indirectly through the synthesis and secretion of prostaglandin E_2 (40).

Our results demonstrating that activation of c-Fos in ARC POMC neurons and increased release of α-MSH from hypothalamic explants in response to IL-1β is decreased but not completely blocked in the presence of a cyclooxygenase inhibitor suggest that activation of these neurons can occur via prostaglandin-independent mechanisms. IL-1β has also been shown to alter the membrane potential and firing rates of neurons in the anterior hypothalamus via prostaglandin E2-independent regulation of γ-aminobutyric acid neurons that project onto these neurons (41). Future studies will be necessary to determine the potential role that these indirect mechanisms may play in mediating the observed effects of IL-1β on the membrane potential and firing rates of ARC POMC neurons.

Conflicting data exist concerning the role of the ARC in mediating IL-1β-induced anorexia. One group previously demonstrated that destruction of the ARC, by neonatal monosodium glutamate treatment or knife-cut disruption of vertical projections from the ARC to the paraventricular nucleus, resulted in augmented anorexia in response to IL-1β (3). Although data from these experiments do not support our model of increased hypothalamic melanocortin signaling mediating IL-1β-induced anorexia, it is important to highlight important caveats of these two paradigms in the context of our results. First, both experimental paradigms would result in substantial disruption of numerous ARC neuropeptide systems. Of particular significance are AgRP neurons, which coexpress NPY and make synaptic contact with POMC neurons, forming a complex neural network whose interplay produces both anorexic and orexigenic effects (42). ARC AgRP/NPY neurons express c-Fos in response to peripheral IL-1β administration (3), and central injections of both NPY and AgRP have been shown to reverse IL-1β-induced anorexia (34, 43). Second, as discussed by the manuscript's authors, ablation of the ARC by monosodium glutamate failed to completely eliminate all IL-1β-sensitive POMC-expressing neurons in the hypothalamus. The combined ability of these neurons to be activated by IL-1β coupled with an impaired or absent compensatory AgRP/NPY response could allow sufficient MC4R activation to drive the observed heightened anorexia. Further characterization of the response of ARC AgRP/NPY neurons to IL-1β may prove essential in resolving this apparent conflict and elucidating the integrated effect of IL-1β on the POMC-AgRP/NPY neural network.

In summary, our results suggest that the hypothalamic melanocortin system is an important target for IL-1β signaling in the brain. The data presented here argue that IL-1β has a predominately stimulatory effect on the activity of the hypothalamic melanocortin system and that increased hypothalamic melanocortin signaling may play a key role in mediating the acute behavioral effects of IL-1β. The observation that IL-1R knockout mice are obese (44) indicates that this system may also play a tonic role in body weight regulation and also provide a mechanism for anorexia and weight loss in both acute and chronic disease states.

Acknowledgments

We thank Maria Glavas, Pushpa Sinnayah, Aaron Eusterbrock, and Gregor Brookhart for technical assistance.

Received January 11, 2007. Accepted May 17, 2007.

Address all correspondence and requests for reprints to: Daniel L. Marks, M.D., Ph.D., Center for the Study of Weight Regulation and Associated Disorders, Oregon Health and Science University, 3181 Southwest Sam Jackson Park Road, Portland, Oregon 97239. E-mail: marksd@ohsu.edu; or Michael A. Cowley, Ph.D., Division of Neuroscience, Oregon National Primate Research Center, Beaverton, Oregon 97006. E-mail: cowleym@ohsu.edu.

This work was supported by Grants National Institute of Diabetes and Digestive and Kidney Diseases (NIDDK) DK 70333 and NIDDK DK 62207 (D.L.M), National Institutes of Health RR00163 and NIDDK DK62202 (M.A.C.), and an American Heart Association Predoctoral Fellowship 0515502Z (J.M.S.).

Disclosure summary: J.M.S., E.E.J., P.J.E., D.D.B., A.K.B., W.F.G., and D.L.M. have no conflicts of interest to declare. Oregon Health and Science University (OHSU) and M.A.C. have a significant financial interest in Orexigen Therapeutics Inc., a company that may have a commercial interest in the results of this research and technology. This potential conflict has been reviewed and managed by the OHSU Conflict of Interest in Research Committee and the Integrity Program Oversight Council.

References

1. **Hart BL** 1988 Biological basis of the behavior of sick animals. Neurosci Biobehav Rev 12:123–137
2. **Elmquist JK, Scammell TE, Saper CB** 1997 Mechanisms of CNS response to systemic immune challenge: the febrile response. Trends Neurosci 20:565–570
3. **Reyes TM, Sawchenko PE** 2002 Involvement of the arcuate nucleus of the hypothalamus in interleukin-1-induced anorexia. J Neurosci 22:5091–5099
4. **Plata-Salaman C, Turrin N** 1999 Cytokine action in the brain. Mol Psychiatry 4:302
5. **Hart BL** 1990 Behavioral adaptations to pathogens and parasites: five strategies. Neurosci Biobehav Rev 14:273–294
6. **Murray MJ, Murray AB** 1979 Anorexia of infection as a mechanism of host defense. Am J Clin Nutr 32:593–596
7. **Ramos EJ, Suzuki S, Marks D, Inui A, Asakawa A, Meguid MM** 2004 Cancer anorexia-cachexia syndrome: cytokines and neuropeptides. Curr Opin Clin Nutr Metab Care 7:427–434
8. **Cone RD** 2005 Anatomy and regulation of the central melanocortin system. Nat Neurosci 8:571–578
9. **Jacobowitz DM, O'Donohue TL** 1978 α-Melanocyte stimulating hormone: immunohistochemical identification and mapping in neurons of rat brain. Proc Natl Acad Sci USA 75:6300–6304
10. **Haskell-Luevano C, Chen P, Li C, Chang K, Smith MS, Cameron JL, Cone RD** 1999 Characterization of the neuroanatomical distribution of agouti-related protein immunoreactivity in the rhesus monkey and the rat. Endocrinology 140:1408–1415
11. **Huszar D, Lynch CA, Fairchild-Huntress V, Dunmore JH, Fang Q, Berkemeier LR, Gu W, Kesterson RA, Boston BA, Cone RD, Smith FJ, Campfield LA, Burn P, Lee F** 1997 Targeted disruption of the melanocortin-4 receptor results in obesity in mice. Cell 88:131–141
12. **Baskin DG, Hahn TM, Schwartz MW** 1999 Leptin sensitive neurons in the hypothalamus. Horm Metab Res 31:345–350
13. **Cowley MA, Smith RG, Diano S, Tschop M, Pronchuk N, Grove KL, Strasburger CJ, Bidlingmaier M, Esterman M, Heiman ML, Garcia-Segura LM, Nillni EA, Mendez P, Low MJ, Sotonyi P, Friedman JM, Liu H, Pinto S, Colmers WF, Cone RD, Horvath TL** 2003 The distribution and mechanism of action of ghrelin in the CNS demonstrates a novel hypothalamic circuit regulating energy homeostasis. Neuron 37:649–661
14. **Niswender KD, Baskin DG, Schwartz MW** 2004 Insulin and its evolving partnership with leptin in the hypothalamic control of energy homeostasis. Trends Endocrinol Metab 15:362–369
15. **Zhang F, Chen Y, Heiman M, Dimarchi R** 2005 Leptin: structure, function and biology. Vitam Horm 71:345–372
16. **Mercer JG, Hoggard N, Williams LM, Lawrence CB, Hannah LT, Trayhurn P** 1996 Localization of leptin receptor mRNA and the long form splice variant (Ob-Rb) in mouse hypothalamus and adjacent brain regions by in situ hybridization. FEBS Lett 387:113–116
17. **Cheung CC, Clifton DK, Steiner RA** 1997 Proopiomelanocortin neurons are direct targets for leptin in the hypothalamus. Endocrinology 138:4489–4492
18. **Dantzer R** 2001 Cytokine-induced sickness behavior: where do we stand? Brain Behav Immun 15:7–24
19. **Rothwell NJ, Luheshi G** 1994 Pharmacology of interleukin-1 actions in the brain. Adv Pharmacol 25:1–20
20. **Plata-Salaman CR** 1998 Cytokine-induced anorexia. Behavioral, cellular, and molecular mechanisms. Ann NY Acad Sci 856:160–170
21. **Ericsson A, Kovacs KJ, Sawchenko PE** 1994 A functional anatomical analysis

of central pathways subserving the effects of interleukin-1 on stress-related neuroendocrine neurons. J Neurosci 14:897–913
22. **Kent S, Bluthe RM, Dantzer R, Hardwick AJ, Kelley KW, Rothwell NJ, Vannice JL** 1992 Different receptor mechanisms mediate the pyrogenic and behavioral effects of interleukin 1. Proc Natl Acad Sci USA 89:9117–9120
23. **Labow M, Shuster D, Zetterstrom M, Nunes P, Terry R, Cullinan EB, Bartfai T, Solorzano C, Moldawer LL, Chizzonite R, McIntyre KW** 1997 Absence of IL-1 signaling and reduced inflammatory response in IL-1 type I receptor-deficient mice. J Immunol 159:2452–2461
24. **Ericsson A, Liu C, Hart RP, Sawchenko PE** 1995 Type 1 interleukin-1 receptor in the rat brain: distribution, regulation, and relationship to sites of IL-1-induced cellular activation. J Comp Neurol 361:681–698
25. **Lawrence CB, Rothwell NJ** 2001 Anorexic but not pyrogenic actions of interleukin-1 are modulated by central melanocortin-3/4 receptors in the rat. J Neuroendocrinol 13:490–495
26. **Cowley MA, Smart JL, Rubinstein M, Cerdan MG, Diano S, Horvath TL, Cone RD, Low MJ** 2001 Leptin activates anorexigenic POMC neurons through a neural network in the arcuate nucleus. Nature 411:480–484
27. **Ellacott KL, Halatchev IG, Cone RD** 2006 Characterization of leptin-responsive neurons in the caudal brainstem. Endocrinology 147:3190–3195
28. **Paxinos G, Franklin K** 2001 The mouse brain in stereotaxic coordinates. 2nd ed. Orlando, FL: Academic Press
29. **Cunningham MJ, Scarlett JM, Steiner RA** 2002 Cloning and distribution of galanin-like peptide mRNA in the hypothalamus and pituitary of the macaque. Endocrinology 143:755–763
30. **Paxinos G, Watson C** 1998 The rat brain in stereotaxic coordinates. 4th ed. Orlando, FL: Academic Press
31. **Cartmell T, Southgate T, Rees GS, Castro MG, Lowenstein PR, Luheshi GN** 1999 Interleukin-1 mediates a rapid inflammatory response after injection of adenoviral vectors into the brain. J Neurosci 19:1517–1523
32. **Inui A** 1999 Cancer anorexia-cachexia syndrome: are neuropeptides the key? Cancer Res 59:4493–4501
33. **Wisse BE** 2004 The inflammatory syndrome: the role of adipose tissue cytokines in metabolic disorders linked to obesity. J Am Soc Nephrol 15:2792–2800
34. **Joppa MA, Ling N, Chen C, Gogas KR, Foster AC, Markison S** 2005 Central administration of peptide and small molecule MC4 receptor antagonists induce hyperphagia in mice and attenuate cytokine-induced anorexia. Peptides 26:2294–2301
35. **Ek M, Kurosawa M, Lundeberg T, Ericsson A** 1998 Activation of vagal afferents after intravenous injection of interleukin-1β: role of endogenous prostaglandins. J Neurosci 18:9471–9479
36. **Fan W, Ellacott KL, Halatchev IG, Takahashi K, Yu P, Cone RD** 2004 Cholecystokinin-mediated suppression of feeding involves the brainstem melanocortin system. Nat Neurosci 7:335–336
37. **Bluthe RM, Michaud B, Kelley KW, Dantzer R** 1996 Vagotomy attenuates behavioural effects of interleukin-1 injected peripherally but not centrally. Neuroreport 7:1485–1488
38. **Ericsson A, Arias C, Sawchenko PE** 1997 Evidence for an intramedullary prostaglandin-dependent mechanism in the activation of stress-related neuroendocrine circuitry by intravenous interleukin-1. J Neurosci 17:7166–7179
39. **Elander L, Engstrom L, Hallbeck M, Blomqvist A** 2006 IL-1β and LPS induce anorexia by distinct mechanisms differentially dependent on microsomal prostaglandin E synthase-1. Am J Physiol Regul Integr Comp Physiol 292: R258–R267
40. **Ferri CC, Yuill EA, Ferguson AV** 2005 Interleukin-1β depolarizes magnocellular neurons in the paraventricular nucleus of the hypothalamus through prostaglandin-mediated activation of a non selective cationic conductance. Regul Pept 129:63–71
41. **Tabarean IV, Korn H, Bartfai T** 2006 Interleukin-1β induces hyperpolarization and modulates synaptic inhibition in preoptic and anterior hypothalamic neurons. Neuroscience 141:1685–1695
42. **Cowley MA, Pronchuk N, Fan W, Dinulescu DM, Colmers WF, Cone RD** 1999 Integration of NPY, AGRP, and melanocortin signals in the hypothalamic paraventricular nucleus: evidence of a cellular basis for the adipostat. Neuron 24:155–163
43. **Sonti G, Ilyin SE, Plata-Salaman CR** 1996 Neuropeptide Y blocks and reverses interleukin-1β-induced anorexia in rats. Peptides 17:517–520
44. **Garcia MC, Wernstedt I, Berndtsson A, Enge M, Bell M, Hultgren O, Horn M, Ahren B, Enerback S, Ohlsson C, Wallenius V, Jansson JO** 2006 Mature-onset obesity in interleukin-1 receptor I knockout mice. Diabetes 55:1205–1213

***Endocrinology* is published monthly by The Endocrine Society (http://www.endo-society.org), the foremost professional society serving the endocrine community.**